

AI HEART DISEASE PREDICTION SYSTEM USING MULTI ATLAS SEGMENTATION

^[1]Arun Inigo.S, ^[2]Shanmugavalli.T, ^[3]Maheswari.G, ^[4]Anand.P

^[1] ^[2] ^[3] ^[4]Assistant Professor, Department Of Computer Science,

^[1] ^[2] ^[3] ^[4] Sethu Institute of Technology, Madurai, Tamilnadu.

ABSTRACT

The evaluation of ventricular function is important for the diagnosis of cardiovascular diseases. It typically involves measurement of the left ventricular (LV) mass and LV cavity volume. Manual delineation of the myocardial contours is time-consuming and dependent on the subjective experience of the expert observer. In this paper, a multi-atlas method is proposed for cardiac magnetic resonance (MR) image segmentation. The Proposed method is novel in two aspects. First, it formulates a patch-based label fusion model in a Bayesian framework. Second, it improves image registration accuracy by utilizing label information, which leads to improvement of segmentation accuracy. The Proposed method was evaluated on a cardiac MR image set of 28 subjects. However, in reality, image registration may not be perfect. If there is slight spatial mismatch between the target image and the warped atlas image, then the target voxel may correspond to a shifted position in the atlas. To account for this registration error, we consider a number of voxels in a local neighborhood in the atlas, as the potential matches for the target voxel. In addition, we replace the voxels by patches since the computation of intensity similarity based on a patch may be more robust than that based on a single voxel. The label in the target image is determined by comparing the target patch to atlas patches and then combining the patch labels.

1. Introduction

We proposed in this paper, the evaluation of ventricular function is important for the diagnosis of cardiovascular diseases, such as hypertrophic cardiomyopathy (HCM), ischemic heart disease (IHD), arrhythmogenic right ventricular dysplasia (ARVD), etc. The evaluation normally involves the measurement of ventricular mass (VM), end-diastolic volume (EDV), and end-systolic volume (ESV) from cardiac MR images. The parameter mainly relies on manual delineation of the myocardial contours, which is time-consuming and dependent on the observer's experience. So a great number of semi-automatic or automatic approaches have been developed for cardiac image segmentation. Multi-atlas segmentation has been demonstrated to significantly improve segmentation accuracy compared to segmentation based on a single atlas. The target image to be segmented is registered to each atlas and the propagated labels from multiple atlases are combined to form consensus segmentation. This method has two advantages compared to single atlas propagation. First, it accounts for the anatomical shape variability by using multiple atlases.

Second, it is robust because segmentation errors associated with single atlas propagation can be averaged out when combining multiple atlases. The consensus segmentation is less likely to be affected, when an individual atlas does not match the target image well or when serious registration errors occur for an individual atlas. Its performance can be improved by selecting a subset of atlases which look more similar to the target image than the other images. So we have implemented Multi atlas segmentation has been demonstrated to significantly improve segmentation accuracy compared to segmentation based on a single atlas. To improve the performance of the patch-based segmentation method and to apply it to various images. We have found that registration accuracy has a great impact on segmentation performance. To solve this alternating optimization problem is able to improve performance compared to the conventional label fusion method. Hypertrophic cardiomyopathy (HCM) is a common genetic heart disorder (affecting almost 1 in 500 people) that can cause several varieties of heart problems not the least of which is sudden death. HCM is a form of heart muscle disease in which the muscular walls of the ventricles (lower chambers of the heart) become abnormally thickened. The thickening of the heart muscle causes the muscle itself to function abnormally. The thickening also can cause the ventricles to become distorted, which can interfere with the function of the aortic valve and the mitral valve, disrupting the flow of blood through the heart. Fortunately, most people with HCM turn out to have a relatively benign form of the disease, and many can live normal or nearly normal lives. However, in some patients with this condition, serious cardiac problems can develop.

There are four kinds of cardiac problems caused by HCM:

1) *HCM can cause diastolic dysfunction.* "[Diastolic dysfunction](#)" refers to the fact that thickened ventricles become stiff, making it more difficult for the ventricles to fill with blood. This stiffness causes the blood to "back up" into the lungs, causing shortness of breath – usually with exertion. The diastolic dysfunction also makes it more difficult for patients with HCM to have arrhythmias, especially a trial fibrillation.

2) *HCM can cause systolic dysfunction.* "Systolic dysfunction" means that the heart's pumping action is not normal - that is, when the heart beats, an insufficient volume of blood is ejected. In HCM, systolic dysfunction is often caused by an obstruction to the flow of blood through the left ventricle, produced by the thickened heart muscle just below the aortic valve.

In contrast our model constructs the relationship between target patch and atlas patches by introducing an auxiliary mapping field and analytically derives a solution to the maximization of a posteriori probability (MAP) problem. In addition, our model considers not only patch-based similarity, but also accounts for the registration uncertainty between target and atlas, which also has an impact on label fusion. The second contribution of this paper is that we improve the registration accuracy for each atlas by incorporating intermediate label information into image registration. We refer to this strategy as "registration refinement."

The underlying rationale is that we regard multi-atlas label fusion as a classifier ensemble, in which each atlas acts as a classifier and the opinions from all the atlases are fused. Intuitively, if the registration performance of each atlas can be improved, the classifier ensemble should also perform better. Some groups have proposed to use non rigid registration instead of affine registration in patch-based label fusion.

2. Literature Review

There are many literature contributions to heart disease diagnoses using data mining and machine learning techniques [11]. Reddy et al. [12] used RF, SVM, NB, NN, and KNN with multiple feature selection such as correlation matrix, recursive feature elimination (RFE), and learning vector quantization (LVQ) model to classify the cardiac disease into normal or abnormal. The results show that RF accomplished the optimal performance. Atallah and Al-Mousa [13] utilized stochastic gradient descent (SGD), KNN, RF, logistic regression (LR), and voting ensemble learning to predict cardiac diseases. The voting ensemble learning model has achieved the best accuracy of 90%. Pillai et al. [14] used a recurrent neural network (RNN), a genetic algorithm, and K-mean to predict heart diseases. RNN has achieved the highest accuracy, and K-mean has achieved the lowest accuracy. Kannan and Vasanthi [15] used four machine learning algorithms: LR, RF, SVM, and stochastic gradient boosting (SGB) to predict heart diseases. The model prediction showed that LR has a best accuracy of 86.5%. Raza [16] applied an ensemble learning model, multilayer perceptron, LR, and NB to classify heart diseases.

The result shows that ensemble learning has improved the prediction performance of cardiac disease compared to other algorithms. Oo and Win [17] used feature subset selection (CFS) with sequential minimal optimization (SMO) to predict heart diseases. The result shows that the CFS-SMO algorithm has achieved the best accuracy 86.96%. Nalluri et al. [18] used two techniques (XGBoost and LR) to improve heart disease prediction. The result showed that LR with an accuracy of 85.68% was better than XGBoost, which achieved an accuracy of 84.46%. Bhat et al. [19] proposed a model that is a combination of multilayer perceptron network (MLP) with a backpropagation algorithm to diagnose heart disease. The result shows that the proposed model has reduced error and an improved accuracy of 80.99%.

Abushariah et al. utilized [20] ANN and adaptive neurofuzzy inference system (ANFIS) to predict cardiac disease. ANN has an obtained optimal accuracy of 87.04%, but ANFIS has achieved the lowest accuracy of 75.93%. Hasan et al. [21] utilized MLP with backpropagation and SVM to classify heart disease. The result showed that MLP achieved the highest accuracy of 98%. Chen et al. [22] used ANN with multiple features to diagnose cardiac disease. The results showed that ANN achieved the best accuracy of 80%. Sonawane and Patil [23] used vector quantization algorithm neural network to predict heart disease. Sapra et al. [24] utilized two datasets (Z-Alizadeh Sani and Cleveland heart disease dataset) that were trained by six machine learning algorithms (LR, deep learning (DL), DT, RF, SVM, and ensemble learning (gradient boosted tree)) to classify cardiac diseases. The results showed that gradient boosted tree achieved the best accuracy of 84% compared to other algorithms.

Haq et al. [25] used seven machine learning algorithms: LR, ANN, KNN, NB, SVM, DT, and RF with three feature selections: minimal-redundancy-maximal-relevance (mRMR), Relief, and Shrinkage and Selection Operator (LASSO) to predict heart disease. LR with Relief achieved the highest accuracy of 89% compared to other techniques.

Patch-based segmentation, most of the efforts has been focused on improving the strategy for patch weight estimation or customizing the patch-based method to specific applications. The existing system has systematic errors so cannot able to identify the error detection and error correction. Patch-based segmentation performance is low. Alternating optimization may not converge to the same solution as the original problem. In existing system has some problem on registration refinement and label fusion.

3. Proposed System for Heart Disease Prediction

In our model considers not only patch-based similarity, and also to solve the impact on label fusion. To improve image registration accuracy by utilizing label information, this leads to improvement of segmentation accuracy. Multi atlas segmentation has been demonstrated to significantly improve segmentation accuracy compared to segmentation based on a single atlas. To improve the performance of the patch-based segmentation method and to apply it to various images. We have found that registration accuracy has a great impact on segmentation performance. To solving this alternating optimization problem is able to improve performance compared to the conventional label fusion method.

3.1. Data Collection.

The heart disease dataset [26] is utilized for training and evaluating models. It consists of 1025 records, 13 features, and one target column. -e target column includes two classes: 1 indicates heart diseases, and 0 indicates nonheart disease. Table 1 describes the details of the features.

3.2 Invert To Colored Image.

All the input images are converted into the gray scale image. Then the gray scale images are invert into the colored image because then only we to get a clear view to detect the MR image problem. We introduce a general technique for “colorizing” grayscale images by transferring color between a source, color image and a destination, grayscale image. Rather than choosing RGB colors from a palette to color individual components, we transfer the entire color “mood” of the source to the target image by matching luminance and texture information between the images. We choose to transfer only chromatic information and retain the original luminance values of the target.

In this section, we describe the general algorithm for transferring color; the basic idea is then extended to use swatches. The general procedure for color transfer requires a few simple steps. First each image is converted into the l color space.

We use jittered samplings select a small subset of pixels in the color image as samples. Next, we go through each pixel in the grayscale image in scan-line order and select the best matching sample in the color image using neighborhood statistics. The best match is determined by using a weighted average of pixel luminance and the neighborhood statistics. The chromaticity values (channels) of Thebes's matching pixel are then transferred to the grayscale image to form the final image.

3.3 Markov Random Field (MRF).

Many vision tasks are naturally posed as energy minimization problems on a rectangular grid of pixels, where the energy comprises a data term and a smoothness term:

$$E(u) = E_{data}(u) + E_{smoothness}(u) .$$

The data term $E_{data}(u)$ expresses our goal that the optimal model u be consistent with the measurements. The smoothness energy $E_{smoothness}(u)$ is derived from our prior knowledge about plausible solutions.

Denoising:

Given a noisy image $I(x, y)$, where some measurements may be missing, recover the original image $I(x, y)$, which is typically assumed to be smooth.

Stereo Disparity:

Given two images of a scene, find the binocular disparity at each pixel, $d(x, y)$. The disparities are expected to be piecewise smooth since most surfaces are smooth.

Surface Reconstruction: Given a sparse set of depth measurements and/or normal's, recover a smooth surface $z(x, y)$ consistent with the measurements.

Segmentation: Assign labels to pixels in an image, e.g., to segment foreground from background.

A Markov Random Field (MRF) is a graph $G = (V, E)$.

- $V = \{1, 2, \dots, N\}$ is the set of nodes, each of which is associated with a random variable (RV), u_j , for $j = 1 \dots N$.
- The neighbourhood of node i , denoted N_i , is the set of nodes to which i is adjacent; i.e., $j \in N_i$ if and only if $(i, j) \in E$.
- The Markov Random field satisfies N_i is often called the Markov blanket of node i .

$$p(u_i | \{u_j\}_{j \in V \setminus i}) = p(u_i | \{u_j\}_{j \in N_i}) .$$

The distribution over an MRF (i.e., over RVs $u = (u_1, \dots, u_N)$) that satisfies (1) can be expressed as the product of (positive) potential functions defined on maximal cliques of G .

Such distributions are often expressed in terms of an energy function E , and clique potentials Ψ_c

$$p(u) = \frac{1}{Z} \exp(-E(u, \theta)), \quad \text{where } E(u, \theta) = \sum_{c \in \mathcal{C}} \Psi_c(\bar{u}_c, \theta_c).$$

Here,

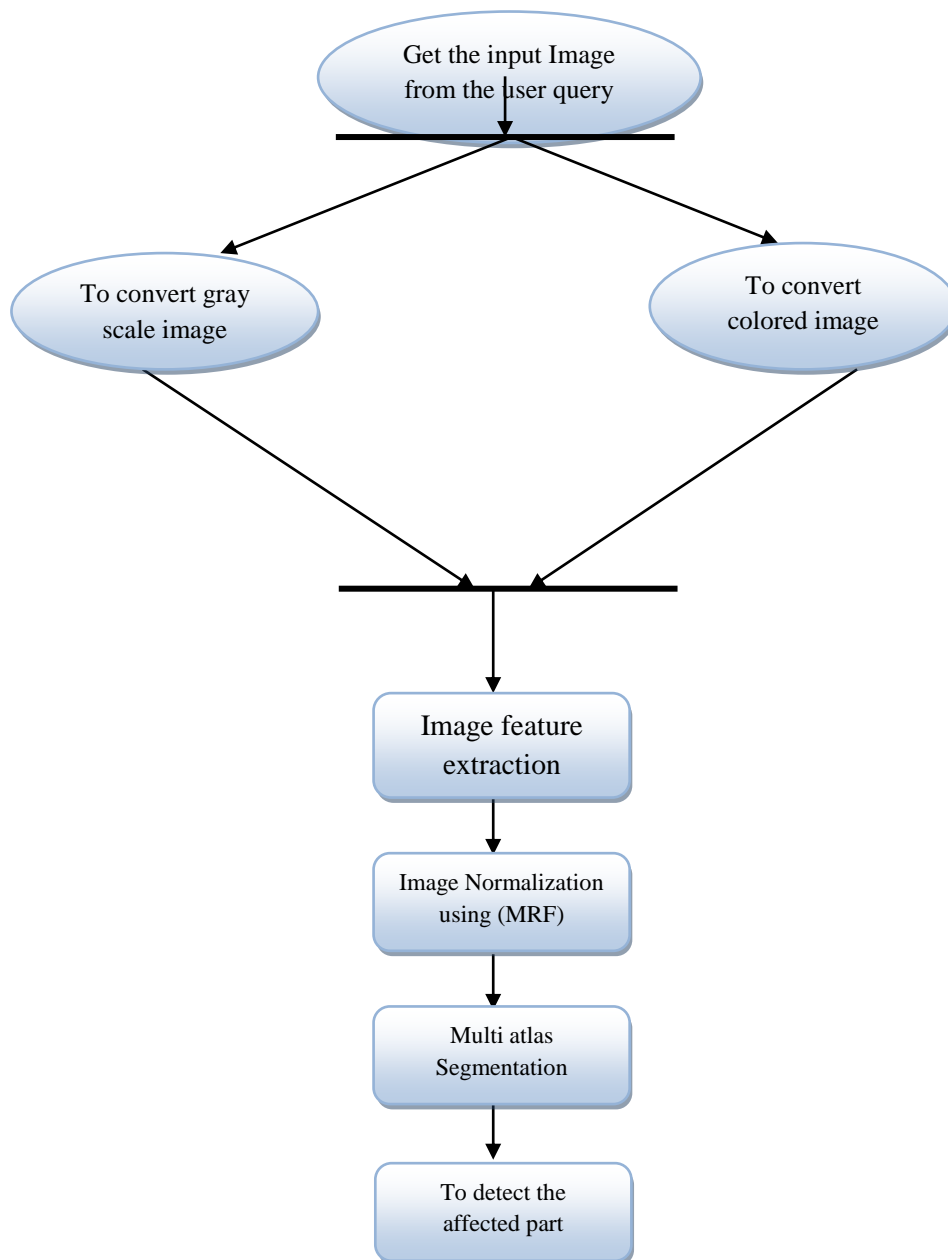
- \mathcal{C} is the set of maximal cliques of the graph (i.e., maximal sub-graphs of G that are fully connected),
- The clique potential Ψ_c , $c \in \mathcal{C}$, is a non-negative function defined on the RVs in clique \bar{u}_c , parameterized by θ_c .
- Z , the partition function, ensures the distribution sums to 1:
-

$$Z = \sum_{u_1 \dots u_N} \prod_{c \in \mathcal{C}} \exp(-\Psi_c(\bar{u}_c, \theta_c))$$

The partition function is important for learning as it's a function of the parameters $\theta = \{\theta_c\}_{c \in \mathcal{C}}$. But often it's not critical for inference.

Inference with MRFs is challenging as useful factorizations of the joint distribution, like those for chains and trees are not available. For all but a few special cases, MAP estimation is NP-hard.

Architecture Diagram:



4. Experimental Results

This section includes a discussion of the experimental results of classification algorithms.

4.1. Experimental Setup.

The experimental results have been implemented using Matlab. -They have also been executed using Intel (R) Core i7 CPU and 8 GB of memory.

4.2. The Result of Applying Feature Selection Methods

4.3 Image Segmentation with Feature Extraction.

Each image divided in various segmentations, and then, that image segmentation should be mention in each and every feature extraction. So it's shown the graft information. Its help to given in image correct information.

When the input data to an algorithm is too large to be processed and it is suspected to be notoriously redundant (e.g. the same measurement in both feet and meters) then the input data will be transformed into a reduced representation set of features (also named features vector). Transforming the input data into the set of features is called *feature extraction*. If the features extracted are carefully chosen it is expected that the features set will extract the relevant information from the input data in order to perform the desired task using this reduced representation instead of the full size input.

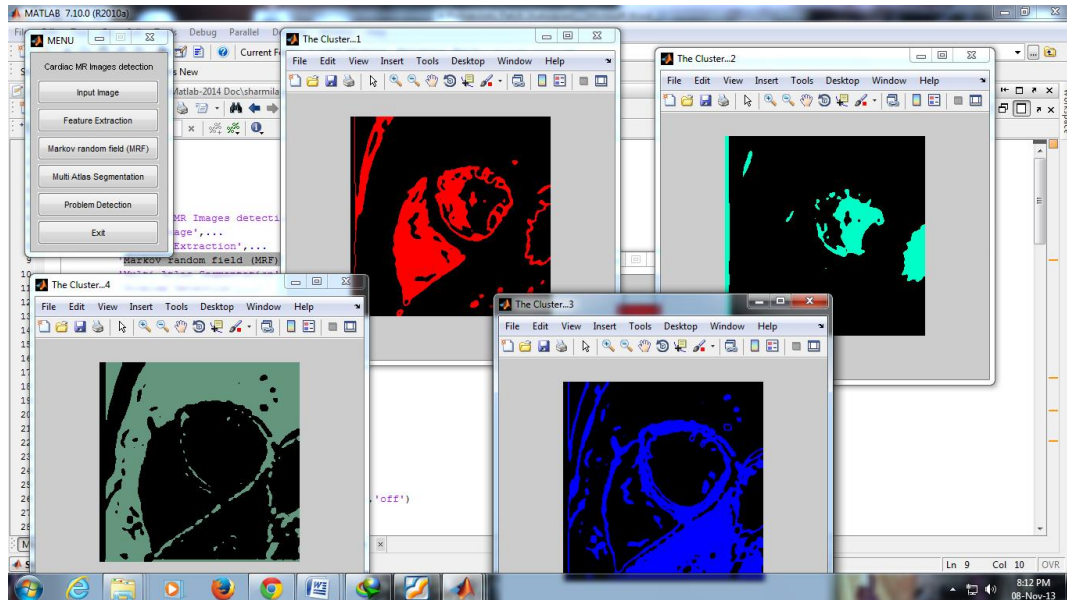
Supervoxel generation and feature extraction To generate supervoxel representations, we apply the efficient graph-based segmentation technique to oversegment images into homogeneous regions. groups neighboring voxels based on their intensity differences, such that similar voxels are more likely to be grouped together. Since for the tumor segmentation problem addressed in our experiments, multi-modality magnetic resonance (MR) images, including T1, contrast-enhanced T1, T2, and FLAIR, are available,

It define intensity difference between two neighboring voxels as the maximal absolute intensity difference between them in all modality channels. In addition, we specify the minimal region size in the resulting oversegmentation to be 100 voxels. These parameters were chosen so that about 1000~2000 supervoxels are produced for each brain image (see Fig. 1 for examples of produced oversegmentations). With such specifications, an image can be segmented within a few seconds on a single 2GHZ CPU.

Before extracting features, we apply image histogram equalization implemented by the *histeq* function in Matlab with default parameters to reduce the intensity scale variations across different subjects. After histogram equalization, the image intensities are normalized into [0; 1] and all processed images have similar intensity histogram profiles.

4.4 Patch Based Multi Atlas Segmentation.

We present the probabilistic patch-based label fusion model. Model assumes that each voxel in the target image is generated from a corresponding voxel in one of the atlases. By introducing this one-to-one mapping from target voxel to atlas voxel, the multi-atlas segmentation problem can be nicely formulated in a framework. So that the mapping from the target voxel to the voxel in the warped atlas is valid.



Supervoxel-based voxel-wise label transfer

Our goal is to find voxel-wise correspondence between a target image and all atlases for label fusion. For this task, we apply image patch based appearance matching. However, directly searching voxel-wise correspondences based on local appearance similarity has limitations. First, local image appearance similarity is not always a reliable indicator for correspondence. Additional regularization constraints, such as smoothness on the correspondence map used in image regis-tration, are often required to make local appearance matching based correspondence searching more reliable. Second, the computation cost for global voxel-wise correspondence searching is too high.

Label fusion

For label fusion, we apply local weighted voting. The fused consensus label prob-ability for a novel target image T_F is obtained by:

$$p(l|x, T_F) = \sum_{j=1}^N w_{x(j)} p(l|x(j), A),$$

where x indexes through all voxels in the target image and l indexes through all possible labels. A is the set of all atlases. $x(j)$ is the j th selected corresponding voxel for x from A using the method described in section 2.2. $p(l|x(j); A)$ is the probability that $x(j)$ votes for label l , which is 1 if $x(j)$ has label l and 0 otherwise.

$w_{x(j)}$ is the voting weights for $x(j)$, with $\sum_{j=1}^N w_{x(j)} = 1$. The consensus segmentation is obtained by selecting the label with the maximal probability for each voxel in the target image. To compute the voting weights, we apply the joint label fusion technique [15], and the solutions are given as:

$$w_x = \frac{M_x^{-1} \mathbf{1}_N}{\mathbf{1}_N^t M_x^{-1} \mathbf{1}_N},$$

$$M_x(j, k) \sim \sum_{m=1}^{L_M} \{|A_F^m(\mathcal{N}(x(j))) - T_F^m(\mathcal{N}(x))|, |A_F^m(\mathcal{N}(x(k))) - T_F^m(\mathcal{N}(x))|\},$$

In our experiments, we applied a patch size $5 \times 5 \times 5$. $\langle \cdot; \cdot \rangle$ is the dot product. LM is the total number of modality channels.

Label fusion at the supervoxel level

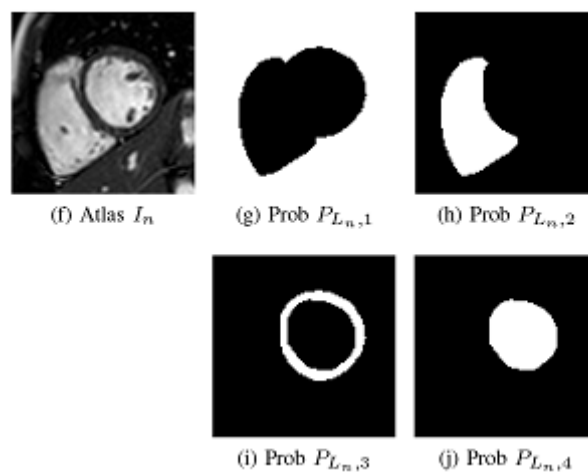
In our experiments, we compare our voxel-wise label transfer and fusion approach with the standard supervoxel-wise label transfer and fusion approach. For supervoxel-wise label fusion, we compute the label distribution of all voxels within an atlas supervoxel to represent its label votes. As in we apply majority voting to fuse the votes from the K selected corresponding supervoxels. The label that has the greatest consensus vote is assigned to all voxels within the target supervoxel.

Machine learning based error correction

Multi-atlas segmentation may produce systematic segmentation errors with respect to manual segmentation. We apply the technique described in to train AdaBoost classifiers to automatically correct systematic errors produced by our multi-atlas segmentation method on a voxel by voxel basis.

4.5 To Detect the Affected Part.

In this section, we present the registration method which estimates the transformation between the target image and the atlas. In case some image should not be encoded in this proposed, it will be save that image segmentations.



Future period, some image will be came in it has been shown the image. Its help to given in correct information. It has been shown that incorporating label information into the registration measure can significantly improve registration accuracy and correct information. And to detect the problems using the multi atlas segmented image. It split into various types of segmented images.

Techniques	Accuracy (%)	Recall (%)	Precision (%)	F-measure (%)	AUC (%)
KNN ($K = 1$)	98.1	98.5	98	98.2	98.5
SVM	85	94.9	79.9	86.7	89.2
DT	98.1	98.5	98	98.2	98.1
MRF	98.2	98.5	98	98.2	98.2
NB	86.7	90	85	87.6	93

Classification performance of applying boosting technique

to selected features by LAD.

In Above Table, MRF has reported the best performance among other algorithms with an accuracy of 98.2%, 98.5% recall, 98.2% AUC, and 98% precision. In contrast, SVM has registered the lowest performance with 85% accuracy, 94.9% recall, 79.9% precision, and 89.2% AUC. The optimal result of KNN when $k = 1$ is 98.1% accuracy. The classification accuracy of NB is 86.7%, 90% recall, and 85% precision. DT achieved 98.1% accuracy, 98.5% recall, 98.1% AUC, and 98% precision. DT and KNN are the second important classification algorithms that have 98.1% accuracy.

5. Conclusion

To conclude, we have proposed a patch-based label fusion model. One of our contributions is that the patch-based model is formulated in a probabilistic MRF method. It is an extension of the probabilistic model in the way that multiple patches, instead of a single voxel, are extracted from each atlas to account for the registration error. In the experiments, we have found that registration accuracy has a great impact on segmentation performance. With registration refinement, label fusion results can be improved. In addition, when registration refinement is used, the difference between different label fusion strategies becomes subtle. Even majority voting can perform quite well in this case. However, if the registration is not very accurate, for example when affine registration is used, sophisticated label fusion strategies such as the patch-based method play a very important role in improving segmentation performance.

6. Future Enhancement

In this project we detect the affected part on a MR image. And to find the connection between the probabilistic label fusion model and the recently proposed patch-based segmentation method. Another contribution is that label information is incorporated into image registration to improve registration accuracy. Experimental results show that registration refinement improves segmentation accuracy. The method produces reliable clinical indexes which are in good agreement with the manual measurements. It can provide useful information for clinicians in cardiac disease diagnosis.

References

- [1] M. Sanz, A. Marco del Castillo, S. Jepsen et al., "Periodontitis and cardiovascular diseases: consensus report," *Journal of Clinical Periodontology*, vol. 47, no. 3, pp. 268–288, 2020.
- [2] World Health Organization. http://www.who.int/cardiocardiovascular_diseases/en. 2019.
- [3] J. Nahar, T. Imam, K. S. Tickle, and Y.-P. P. Chen, "Association rule mining to detect factors which contribute to heart disease in males and females," *Expert Systems with Applications*, vol. 40, no. 4, pp. 1086–1093, 2013.
- [4] S. N. Blair, "Commentary on Wang Y et al. "An Overview of Non-exercise Estimated Cardiorespiratory Fitness: estimation Equations, Cross-Validation and Application"" *Journal of Science in Sport and Exercise*, vol. 1, no. 1, pp. 94-95, 2019.
- [5] K. Vanisree and J. Singaraju, "Decision support system for congenital heart disease diagnosis based on signs and symptoms using neural networks," *International Journal of Computer Application*, vol. 19, pp. 6–12, 2011.
- [6] A.-H. Abdel-Aty, H. Kadry, M. Zidan et al., "A quantum classification algorithm for classification incomplete patterns based on entanglement measure," *Journal of Intelligent and Fuzzy Systems*, vol. 38, no. 9, pp. 1–8, 2020.
- [7] A. Sagheer, M. Zidan, and M. M. Abdelsamea, "A novel autonomous perceptron model for pattern classification applications," *Entropy*, vol. 21, no. 8, p. 763, 2019.
- [8] M. Aljanabi, H. Qutqut, and M. Hijjawi, "Machine learning classification techniques for heart disease prediction: a review," *International Journal of Engineering and Technology*, vol. 7, pp. 5373–5379, 2018.
- [9] T. Obasi and M. O. Shafiq, "Towards comparing and using machine learning techniques for detecting and predicting heart attack and diseases," in *Proceedings of the 2019 IEEE International Conference on Big Data (Big Data)*, pp. 2393–2402, Los Angeles, CA, USA, April 2019.
- [10] A. A. Ali, H. S. Hassan, and E. M. Anwar, "Heart diseases diagnosis based on a novel convolution neural network and gated recurrent unit technique," in *Proceedings of the 2020 12th International Conference on Electrical Engineering (ICEENG)*, vol. 145–150, Cairo, Egypt, July 2020.
- [11] V. Pham, Q. De Hemptinne, J.-M. Grinda et al., "Giant coronary aneurysms, from diagnosis to treatment: a literature review," *Archives of Cardiovascular Diseases*, vol. 113, pp. 59–69, 2020.
- [12] N. S. C. Reddy, S. S. Nee, L. Z. Min, and C. X. Ying, "Classification and feature selection approaches by machine learning techniques: heart disease prediction," *International Journal of Innovative Computing*, vol. 9, 2019.
- [13] R. Atallah and A. Al-Mousa, "Heart disease detection using machine learning majority voting ensemble method," in *Proceedings of the 2019 2nd International Conference on New Trends in Computing Sciences (ICTCS)*, pp. 1–6, Amman, Jordan, October 2019.

- [14] N. S. R. Pillai, K. K. Bee, and J. Kiruthika, "Prediction of heart disease using rnn algorithm," *International Research Journal of Engineering and Technology*, vol. 5, 2019.
- [15] R. Kannan and V. Vasanthi, "Machine learning algorithms with roc curve for predicting and diagnosing the heart disease," *InSoft Computing and Medical Bioinformatics*, pp. 63–72, 2019.
- [16] K. Raza, "Improving the prediction accuracy of heart disease with ensemble learning and majority voting rule," *InUHealthcare Monitoring Systems*, pp. 179–196, 2019.
- [17] A. N. Oo and K. T. Win: Feature Selection Based Sequential Minimal Optimization (Smo) Classifier for Heart Diseaseclassification.
- [18] S. Nalluri, R. V. Saraswathi, S. Ramasubbareddy, K. Govinda, and E. Swetha, "Chronic heart disease prediction using datamining techniques," *InData Engineering and Communication Technology*, pp. 903–912, 2020.
- [19] R. Bhat, S. Chawande, and S. Chadda, "Prediction of test for heart disease diagnosis using artificial neural network," *Indian Journal of Applied Research*, vol. 9, 2019.
- [20] M. A. Abushariah, A. A. Alqudah, O. Y. Adwan et al., "Automatic heart disease diagnosis system based onartificial neural network (ann) and adaptive neuro-fuzzy inference systems (anfis) approaches," *Journal of Software Engineering and Applications*, vol. 7, p. 1055, 2014.
- [21] T. T. Hasan, M. H. Jasim, and I. A. Hashim, "Heart disease diagnosis system based on multi-layer perceptron neural networkand support vector machine," *International Journal of Current Engineering and Technology*, vol. 77, pp. 2277–4106, 2017.
- [22] A. H. Chen, S.-Y. Huang, P.-S. Hong, C.-H. Cheng, and E.-J. Lin, "Hdps: heart disease prediction system," *In 2011 computing in Cardiology*, vol. 557–560, 2011.
- [23] J. S. Sonawane and D. Patil, "Prediction of heart disease using learning vector quantization algorithm," in *Proceedings of the 2014 Conferenceon IT in Business, Industry and Government (CSIBIG)*, vol. 1–5, Indore, India, March 2014.
- [24] L. Sapra, J. K. Sandhu, and N. Goyal, "Intelligent method for detection of coronary artery disease with ensemble approach," *Advances in Communication and Computational Technology*, vol. 1033–1042, 2021.
- [25] A. U. Haq, J. P. Li, M. H. Memon, S. Nazir, and R. Sun, "A hybrid intelligent system framework for the prediction of heartdisease using machine learning algorithms," *Mobile Complexity 9 Information Systems*, vol. 2018, Article ID 3860146, 21 pages, 2018.
- [26] <https://www.kaggle.com/johnsmith88/heart-diseasedataset>.
- [27] C. Ricciardi, A. S. Valente, K. Edmund et al., "Linear discriminant analysis and principal component analysis to predict coronary artery disease," *Health Informatics Journal*, vol. 26, no. 3, pp. 2181–2192, 2020.
- [28] A. K. Garate-Escamilla, A. H. E. Hassani, and E. Andres, "Classification models for heart disease prediction using featureselection and pca," *Informatics Medicine Unlocked*, vol. 19, Article ID 100330, 2020.
- [29] A. A. Ali, H. S. Hassan, and E. M. Anwar, "Improve the accuracy of heart disease predictions using machine learning andfeature selection techniques," in *Proceedings of the*

International Conference on Machine Learning, Image Processing, Network Security and Data Sciences, pp. 214–228, Assam, India, April 2020.